

# PHYSICAL REVIEW A

## GENERAL PHYSICS

THIRD SERIES, VOL. 5, NO. 4

APRIL 1972

### $K\beta/K\alpha$ X-Ray Transition-Probability Ratios for Elements $18 \leq Z \leq 39$ \*

V. W. Slivinsky and P. J. Ebert

Lawrence Livermore Laboratory, University of California, Livermore, California 94550

(Received 27 September 1971)

$K\beta/K\alpha$  x-ray transition-probability ratios for 16 elements in the range  $18 \leq Z \leq 39$  were measured with a high-resolution Si(Li) detector. The  $K$  vacancies were produced by a heavily filtered bremsstrahlung beam from a commercial x-ray tube. Our results agree qualitatively with the theoretical calculations of Scofield but are consistently about 15% higher.

#### I. INTRODUCTION

Several experiments measuring  $K\beta/K\alpha$  x-ray transition-probability ratios have been reported since 1969.<sup>1-3</sup> Theoretical calculations of  $K$  radiative decay rates have also appeared recently.<sup>4-6</sup> While the calculations of  $K\beta/K\alpha$  all agree to within  $\pm 5\%$ , none of the experiments agrees very well with the theory for elements with  $Z \leq 40$ . Furthermore, agreement among the experiments is poor in this region.

One feature of the theoretical curves is that  $K\beta/K\alpha$  is relatively constant for  $21 \leq Z \leq 30$ , where the  $3d$  levels are being filled. The results of Hansen *et al.*,<sup>2</sup> however, show a relatively flat portion of the curve for  $26 \leq Z \leq 33$ ; for elements with  $Z \leq 26$ ,  $K\beta/K\alpha$  decreases more rapidly with decreasing  $Z$  than the theory indicates. Salem and Johnson<sup>7</sup> measured  $(K\beta_1 + K\beta_3)/K\alpha_1$  for elements with  $22 \leq Z \leq 47$  by using electrons to excite thick targets and measuring the x-ray lines with a diffractometer. They report a rapidly increasing ratio with  $Z$  and no flat portion anywhere in this region. Their results favor the theoretical calculations by Babushkin<sup>8</sup> who used a Coulomb potential and found no flat region for  $21 \leq Z \leq 30$ . All of these results are summarized by Nelson *et al.*<sup>9</sup> in a review article.

Our previous experimental results extended down to  $Z = 29$ . They were least accurate for the lowest- $Z$  elements mainly because the  $K\alpha$  and  $K\beta$  peaks were only partially resolved. However, our ratios are 15% higher than those in Refs. 2 and 3 at  $Z = 29, 30$ , and the error limits do not overlap. This work was prompted to resolve this disagreement and also to systematically investigate the low- $Z$  region.

#### II. EXPERIMENT

##### A. Production of $K$ -Shell Vacancies

There are several ways in which  $K$ -shell vacancies can be produced. Electrons can directly excite  $K$ -shell vacancies,<sup>3,7</sup> but a large bremsstrahlung background is produced along with the fluorescent lines. The uncertainty in the subtraction of this background can cause a significant error in the measurement of the lines. Heavy charged particles have also been used to produce  $K$  vacancies.<sup>10</sup> While the bremsstrahlung background is reduced considerably with this mode of excitation, stripping of the outer electrons by a slowly moving charged particle alters the  $K\beta/K\alpha$  ratio and makes comparison with theory difficult. Hansen *et al.*<sup>2</sup> used radioactive isotopes as  $K$  x-ray sources. A radioactive source used for this purpose must be thin to its own fluorescent x rays or be of a known uniform thickness so that the difference in self-absorption at the  $K\alpha$  and  $K\beta$  energies can be accounted for accurately. The source should also decay primarily by  $K$  capture or  $K$  conversion, so that the background near the fluorescent peaks from higher-energy  $\gamma$  rays scattering out of the detector is small. A limited selection of easily produced radioactive isotopes has these properties. For these reasons, we used bremsstrahlung from a heavily filtered Mo-target x-ray tube to produce the  $K$  vacancies. Almost negligible background is present near the fluorescent peaks with this method, and a large number of thin targets covering a wide range of  $Z$  can be used. We used one  $K$ -capture isotope, a thin ( $10^{-6}$  g/cm<sup>2</sup>) <sup>55</sup>Fe source with an activity of  $1 \times 10^{-6}$  Ci, in an attempt to duplicate the method of

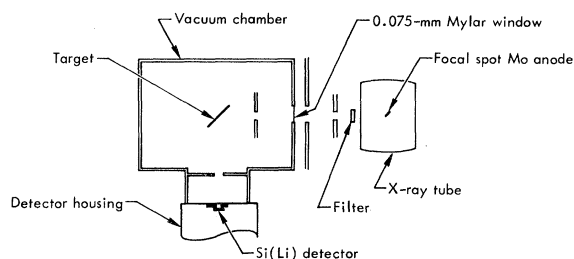


FIG. 1. Experimental configuration.

excitation used by Hansen *et al.*<sup>2</sup>; we compare that result with our other results.

### B. Experimental Configuration

The experimental configuration is shown in Fig. 1. Targets of 16 elements were used; each was placed in the collimated x-ray beam. The solid targets were made by evaporating high-purity metals or compounds on  $2.5 \times 10^{-4}$ -cm-thick Be substrates. The thickness of the targets ranged from  $(40-90) \times 10^{-6}$  g/cm<sup>2</sup>, which is thin enough that there was no significant correction to the data for the difference in self-absorption between the  $K\alpha$  and  $K\beta$  lines. For these targets the system was evacuated to  $10^{-3}$  Torr to eliminate an air-attenuation correction to the data. For  $Z=18$  (Ar) and  $Z=36$  (Kr), the target chamber was filled with high-purity gas to a pressure of 25 Torr.

Since it is possible that the chemical composition of the target might affect the results,<sup>11</sup> we also used thick targets ( $2.5 \times 10^{-3}$  cm) of high-purity Sc, Ti, Cu, and Zn. We compare these results with thin-target results for the same elements.

### C. Si(Li) Spectrometer

The Si(Li) spectrometer with its pulsed-light-feedback preamplifier and a low-noise amplifier was fabricated at the Lawrence Berkeley Laboratory. The Si wafer is approximately 3 mm thick and has a collimated front surface area of 12.3 mm<sup>2</sup>. The vacuum window on the system is high-purity Be whose thickness,  $9.613 \times 10^{-3}$  g/cm<sup>2</sup>, was measured by weighing, and whose purity was checked by measuring its transmission to 4.0-keV x rays and comparing with the calculated transmission using the measured cross section.<sup>12</sup> The Si wafer also has a thin layer of Au, whose thickness is approximately  $1 \times 10^{-6}$  cm on its front surface, and a Si dead layer with a thickness of about  $1 \times 10^{-5}$  cm.<sup>13</sup> This system has a resolution of 195 eV for the 5.9-keV photons of <sup>55</sup>Fe. Counts were recorded on a multichannel analyzer.

The efficiency of the spectrometer was measured between 8 and 25 keV using a technique described elsewhere.<sup>14</sup> This upper-energy calibration deter-

mined the energy at which the Si wafer transmits an appreciable number of incident photons. The Si(Li) detector was found to be totally absorbing<sup>15</sup> up to 15 keV.

The spectrometer was also calibrated at the Sc  $K\alpha$  energy, 4.09 keV, by comparing it with a thin-window gas proportional counter whose efficiency was calculated. The Si(Li) spectrometer was 92% efficient at this energy. Photons absorbed in the Be window account for 7% of this loss, and the other 1% is presumably absorbed in the Au front surface and in the Si dead layer. The attenuation of 4.09-keV photons in  $1 \times 10^{-6}$ -cm Au and  $1 \times 10^{-5}$ -cm Si is calculated to be 3%. Since the accuracy of the calibration was  $\pm 3\%$ , we concluded that the layers of Au and Si were about as thick as stated by the manufacturer. Below 4.09 keV, for the  $Z=18$  and  $Z=19$  fluorescent energies, the efficiency of the spectrometer was calculated using the above layer thicknesses. The data were corrected for the difference in efficiency at the  $K\alpha$  and  $K\beta$  energies.

### III. SPECTRUM ANALYSIS

The x-ray tube was generally run at 30 kV and 75 mA. The bremsstrahlung beam from the tube was filtered with high-purity Al for the low- $Z$  targets and with Mo and high-purity Al for the higher- $Z$  elements. This filtering considerably reduced the scattered background near the fluorescent peaks. Figure 2(a) shows the Zn spectrum plotted on a log scale to emphasize the low background. For the lower- $Z$  elements, tailing in the detector was more significant, as shown in Fig. 2(b). It is important to stress that there is no contribution to the tail from x rays with lower energies than the fluorescent lines because of the heavy filtering of the excitation source. This is also evident from the energy spectrum from the <sup>55</sup>Fe isotope, which decays entirely by  $K$  capture but still shows counts below the photopeaks (see Fig. 3). For the  $K\beta/K\alpha$  measurements, therefore, the background under the photopeaks was determined by the background level just above the  $K\beta$  peak; in most cases, this was about 0.1% of the  $K\beta$  peak height.

The tail counts must be due to incomplete charge collection, and they properly belong in the photopeaks. Since the  $K\alpha$  peak is so much more intense than the  $K\beta$  peak, we could determine the total number of tail counts per photopeak count as a function of x-ray energy (Fig. 4). This curve in Fig. 4 was used to determine the number of tail counts that were added to the  $K\alpha$  and  $K\beta$  photopeaks.

It should be noted in Figs. 2 and 3 that the escape peak associated with the  $K\beta$  photopeak is obscured by the tailing of the  $K\alpha$  peak. To determine what fraction of the  $K\beta$  photons are in its escape peak, we measured the escape peak-to-photopeak ratios for the  $K\alpha$  lines. These results are shown in Fig.

5; the error bars represent the uncertainty due to the statistics in counting the escape peaks. The correction to the  $K\beta/K\alpha$  measurements for the difference in the escape peak-to-photopeak ratio for the  $K\alpha$  and  $K\beta$  energies was less than 0.1% in the worst case and therefore was ignored.

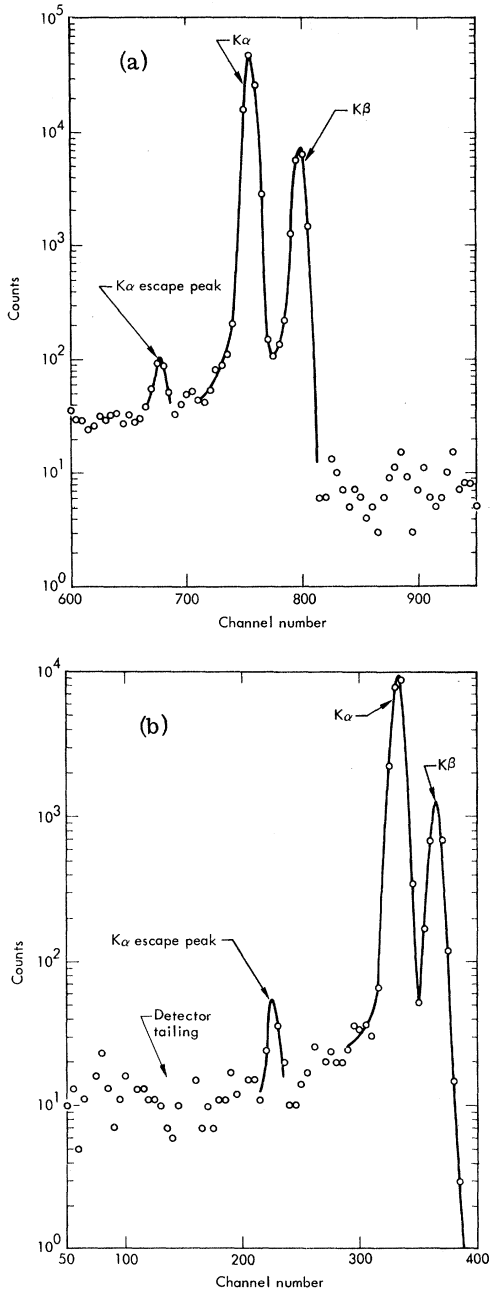


FIG. 2. (a) The energy spectrum from a thin Zn target that is fluoresced with bremsstrahlung from an x-ray tube. (b) The energy spectrum from a thin Cr target. Tailing in the detector becomes significant for the lower- $Z$  elements.

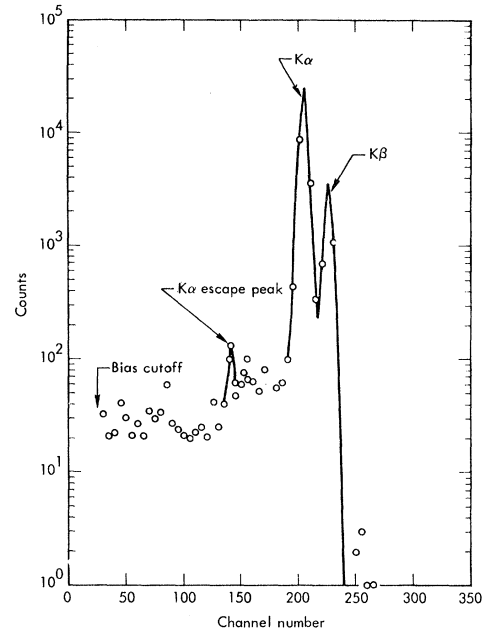


FIG. 3. The energy spectrum from the  $^{55}\text{Fe}$  source.

Of particular concern was the presence of impurities in the Be substrate that might introduce small fluorescent peaks under the peaks of interest. A Be substrate was run without any target material on it. Nanogram quantities of Fe and Mn were found in the Be, but counts from these impurities were negligible when compared with the counts from an actual target.

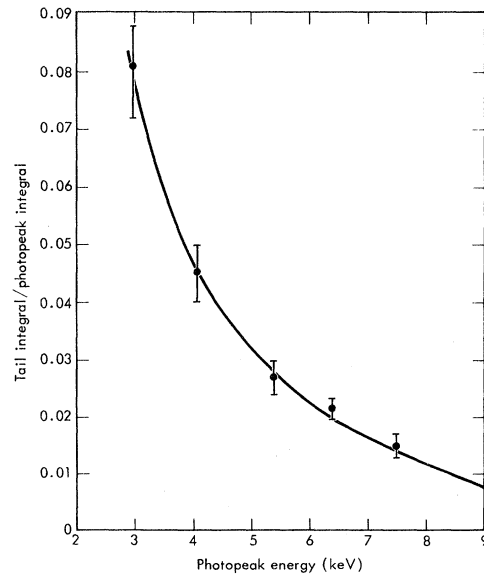


FIG. 4. Total number of counts in the tail per number of counts in the photopeak.

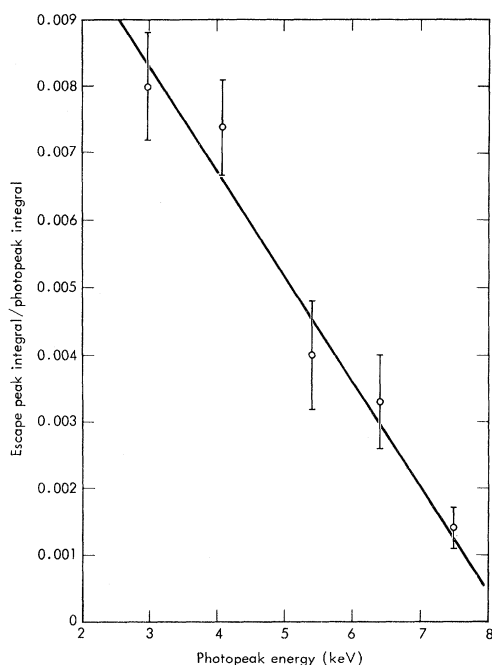


FIG. 5. Escape peak-to-photopeak ratio as a function of photopeak energy.

Finding the peak areas for most elements simply amounted to subtracting the background and then adding the counts in the peaks that were well separated. For the lower- $Z$  elements, however, the  $K\alpha$  and  $K\beta$  peaks were not completely resolved and had to be graphically separated. This was done by constructing similarly shaped peaks whose sum, in all cases, was equal to at least 99.8% of the total number of  $K\alpha$  and  $K\beta$  counts. Spectrometer resolution as a function of photopeak energy was accounted for in this method. For  $Z \geq 21$ , more than 99% of the constructed peak areas was used to de-

TABLE I. Final results of  $K\beta/K\alpha$  measurements.

$Z$	Element	$K\beta/K\alpha$	Hansen <i>et al.</i> (Ref. 2)	Mistry and Quarles (Ref. 3)
18	Ar	$0.1032 \pm 0.0067$		
19	K	$0.1217 \pm 0.0055$		
21	Sc	$0.1302 \pm 0.0026$		
22	Ti	$0.1319 \pm 0.0017$		
23	V	$0.1339 \pm 0.0011$		
24	Cr	$0.1344 \pm 0.0011$	$0.1135 \pm 0.0023$	
25	Mn	$0.1361 \pm 0.0011$		
26	Fe	$0.1366 \pm 0.0011$	$0.1283 \pm 0.0025$	
27	Co	$0.1376 \pm 0.0011$		
28	Ni	$0.1385 \pm 0.0011$		
29	Cu	$0.1387 \pm 0.0011$		$0.1285 \pm 0.0096$
30	Zn	$0.1418 \pm 0.0011$		$0.1330 \pm 0.0084$
32	Ge	$0.1493 \pm 0.0012$		
33	As		$0.1440 \pm 0.0029$	
34	Se	$0.1595 \pm 0.0013$		
36	Kr	$0.1715 \pm 0.0014$		
38			$0.1732 \pm 0.0015$	
39	Y	$0.1842 \pm 0.0015$		

termine  $K\beta/K\alpha$ .

#### IV. RESULTS

Each element from  $Z = 21$  to  $Z = 30$  was run at least three times with greater than  $2 \times 10^4$  counts accumulated in the  $K\beta$  peak. The results for each element were averaged to produce the final value. Elements with  $Z > 32$  were run just once, and for  $Z = 18$  and  $Z = 19$ , where the statistical error was much less than the error associated with separating the peaks, each element was run twice. All of the aforementioned corrections to the data were combined to form a total correction factor by which the  $K\beta/K\alpha$  data were divided to give the final results. This total correction factor as a function of  $Z$  is shown in Fig. 6.

The  $K\beta/K\alpha$  results are listed in Table I and are shown in Fig. 7. Our previous experimental results<sup>1</sup> are also shown for comparison. The present results are systematically lower than our previous results for elements with  $Z < 35$ . The probable cause for this was that the targets used in the previous experiment were metal oxide powders that had some thick areas where differential absorption was important. No correction was made to those data for differential absorption.

Other experimental results<sup>2,3</sup> are also shown in Fig. 7 along with the  $K\beta/K\alpha$  values calculated by Scofield.<sup>4</sup> It can be seen that the curve drawn through our data points is qualitatively similar to Scofield's curve in that there is a region between  $21 \leq Z \leq 30$  where  $K\beta/K\alpha$  does not change rapidly with  $Z$ . Scofield's calculations show dips at  $Z = 24$  (Cr) and  $Z = 29$  (Cu) where the atom prefers an extra  $3d$  electron rather than two  $4s$  electrons. We studied these two elements very closely, but found no justification from our measurements for departing from the smooth line shown in Fig. 7.

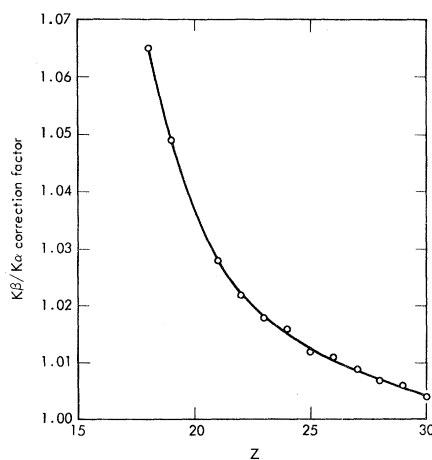


FIG. 6. Correction factor applied to the  $K\beta/K\alpha$  measurements for elements with atomic number  $Z$ .

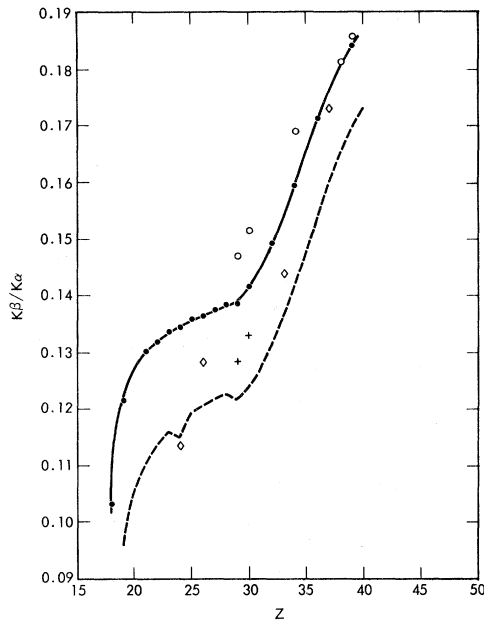


FIG. 7. The  $K\beta/K\alpha$  results as a function of  $Z$ . Qualitatively, the data show the same leveling off at  $Z=21-30$  as calculated by Scofield (Ref. 4). ●, present results; ○, Slivinsky and Ebert (Ref. 1); dashed line, Scofield calculations (Ref. 4); ◇, Hansen *et al.* (Ref. 2); +, Mistry and Quarles (Ref. 3).

The  $K\beta/K\alpha$  result from the experiment using an  $^{55}\text{Fe}$  source and counting the Mn fluorescent lines was  $0.1379 \pm 0.0014$ , while the result from using a Mn fluorescer excited by the bremsstrahlung from the x-ray tube was  $0.1361 \pm 0.0014$ . The measured difference in  $K\beta/K\alpha$  for these two different modes of producing K vacancies in Mn is within the experimental errors of the measurements.

The results from the thick-target experiments were in excellent agreement with the  $K\beta/K\alpha$  values for the thin targets. Even though the correction factors for self-absorption were about 10%, the final results were within 1% of the thin-target results.

## V. ERROR ANALYSIS

Sources of error contributing to the uncertainty in our measured ratios are considered below.

### A. Target Thickness

The difference in self-attenuation for the  $K\alpha$  and  $K\beta$  photons was calculated to be typically 0.07%. The error resulting from this correction is negligible.

### B. Spectrometer Efficiency

It is assumed that the photons that interact in the Si dead layer of the detector are not counted, and the spectrometer efficiency is lowered to account

for this calculated attenuation. If, however, these photons are counted either in the photopeak or in the tail of the spectrum, then an error that ranges from 0.3% at  $Z=18$  to 0.1% at  $Z=25$  is introduced in our  $K\beta/K\alpha$  results.

The thickness of the Au layer on the front surface of the detector is known to  $\pm 20\%$ . The largest correction for differential attenuation of the  $K\alpha$  and  $K\beta$  photons in the Au is 0.5% at  $Z=19$ . Therefore, the largest error in the measured  $K\beta/K\alpha$  from this correction is  $\pm 0.1\%$ .

The uniformity in the thickness of the Be window is estimated to be no worse than  $\pm 10\%$ . The largest correction for differential attenuation in the Be is 5% for  $Z=18$ . Therefore, the largest error is  $\pm 0.5\%$  at  $Z=18$  and decreases to  $\pm 0.1\%$  at  $Z=25$ .

### C. Detector Tailing

Any reasonable curve drawn through the data points in Fig. 4 would not differ from our curve by more than 15%. Since the maximum tailing correction was 0.9%, the maximum error introduced by the correction uncertainty is  $\pm 0.14\%$ .

### D. Background

For most of the measurements, the background was about 0.5% of the  $K\beta$  peak area. Therefore, a 10% statistical uncertainty in the background introduces a 0.1% error due to background subtraction.

### E. Statistics

The statistical error is primarily determined by the number of counts in the  $K\beta$  peak. For each run this error was about 0.7%. Since the final result for most elements was the average of several runs, this error is reduced considerably.

### F. Unresolved Peaks

The standard deviations of the  $K\beta/K\alpha$  measurements for each element between  $Z=22$  and  $Z=30$  ranged from 0.5% to 1%. This indicates that the spread in the data for these elements is primarily due to the statistics mentioned Sec. V E. The standard deviation for elements with  $Z=18$ , 19, and 21 was 3%, which indicates that the error involved with graphically separating the unresolved peaks limits the precision for these elements.

### G. Total Error

The precision of the measurements is the standard deviation given in Sec. V F divided by the square root of the number of measurements. For elements with  $Z \geq 21$ , the precision is 0.3%; for elements with  $Z < 21$ , it is 1.5%.

The accuracy of these measurements for elements with  $Z < 22$  is limited by how many counts can be taken out of (or put into) the  $K\beta$  peak and

still satisfy the graphical separation requirements previously mentioned. This error is estimated to be  $\pm 5\%$  for  $Z=18$ ,  $\pm 3\%$  for  $Z=19$ ,  $\pm 2\%$  for  $Z=21$ , and  $\pm 1\%$  for  $Z=22$ . For elements with  $23 \leq Z \leq 30$ , the errors from sources in Secs. VB-V D were combined to give an accuracy of  $\pm 0.5\%$ ; for  $Z > 30$ , these errors were negligible.

The precision and accuracy were combined linearly to give the total errors quoted in Table I.

## VI. DISCUSSION

This experiment measured  $K\beta/K\alpha$  for 16 elements in the range  $18 \leq Z \leq 39$ . Measurements were made for both thin targets and thick targets, to show that chemical effects, such as an oxidized thin target, did not change the result. For most of the elements, the experimental error from known sources was less than  $\pm 1\%$ . The results form a smoothly varying function with  $Z$  that agrees qualitatively with the calculations by Scofield. The dips in the theoretical curve at  $Z=24$  and  $Z=29$  were not found

here.

Our results are in disagreement with the measurements of Hansen *et al.*,<sup>2</sup> and the two different methods for producing the  $K$ -shell vacancies does not account for the difference between the two measurements. The difference between our results and those of Mistry and Quarles<sup>3</sup> is about 7%. However, their error bars overlap ours.

*Note added in manuscript.* At the completion of this work, a study of  $K$  x-ray intensities by J. H. McCrary *et al.* was called to our attention.<sup>16</sup> Their  $K\beta/K\alpha$  results in the region  $20 \leq Z \leq 39$  are in excellent agreement with those reported herein.

## ACKNOWLEDGMENTS

The authors thank Dr. W. C. Dickinson for his helpful discussions and criticisms. We acknowledge the capable assistance of R. A. Hansen in acquiring the data. We also thank P. H. Jacob for making the thin targets and R. J. Nagle for providing the <sup>55</sup>Fe source.

\*Work performed under the auspices of the U. S. Atomic Energy Commission.

<sup>1</sup>V. W. Slivinsky and P. J. Ebert, Phys. Letters 29A, 463 (1969).

<sup>2</sup>J. S. Hansen, H. U. Freund, and R. W. Fink, Nucl. Phys. A142, 604 (1970).

<sup>3</sup>V. D. Mistry and C. A. Quarles, Nucl. Phys. A164, 604 (1970).

<sup>4</sup>J. H. Scofield, Phys. Rev. 179, 9 (1969).

<sup>5</sup>H. R. Rosner and C. P. Bhalla, Z. Physik 231, 347 (1970).

<sup>6</sup>E. J. McGuire, Phys. Letters 33A, 288 (1970).

<sup>7</sup>S. I. Salem and J. P. Johnson, Phys. Letters 30A, 163 (1969).

<sup>8</sup>F. A. Babushkin, Acta Phys. Polon. 31, 459 (1967).

<sup>9</sup>G. C. Nelson, S. I. Salem, and B. G. Saunders, At.

Data 1, 377 (1970).

<sup>10</sup>A. R. Knudson, D. J. Nagel, P. G. Burkhalter, and K. L. Dunning, Phys. Rev. Letters 26, 1149 (1971).

<sup>11</sup>H. H. Roseberry and J. A. Bearden, Phys. Rev. 50, 204 (1936).

<sup>12</sup>B. L. Henke, Norelco Repr. 14, 118 (1967).

<sup>13</sup>J. Walton, Lawrence Berkeley Laboratory (private communication).

<sup>14</sup>V. W. Slivinsky and P. J. Ebert, Nucl. Instr. Methods 71, 346 (1969).

<sup>15</sup>"Totally absorbing" is defined here as having  $< 1\%$  transmission.

<sup>16</sup>J. H. McCrary, L. V. Singman, L. H. Ziegler, L. D. Looney, C. M. Edmonds, and Carolyn E. Harris, Phys. Rev. A 4, 1745 (1971).